Vietnam Journal of Mechanics, VAST, Vol. 37, No. 2 (2015), pp. 105 – 122
DOI:10.15625/0866-7136/37/2/5552

DYNAMIC RESPONSE OF THREE DIMENSION TUNNEL ON ELASTIC FOUNDATION SUBJECTED TO MOVING VEHICLE LOADS

Nguyen Thai Chung*, Do Ngoc Tien
Le Quy Don Technical University, Hanoi, Vietnam
*E-mail: thaichung1271@gmail.com
Received November 24, 2014

Abstract. Dynamic response analysis of tunnel with elastic foundation subjected to the load such as the hydrostatic pressure, seismic or moving load is an important but complicate problem in transport engineering due to increasing of traffic volume. This paper is devoted to study dynamic response of a tunnel surrounded by elastic foundation under moving vehicle loads by using the finite element method (FEM). The numerical results were then validated by an experimentation on a real structure.

Keywords: Tunnel, moving load, dynamic analysis, experimental testing.

1. INTRODUCTION

Möller et al. [1], Vermeer et al. [2], investigated tunnel structures subjected to static loads in the framework of 3D model and validated then by experimental results. By using finite element method, Hyon et al. [3], Sramoon et al. [4], Hussein and Hunt [5], the tunnel structures subjected to moving load were analyzed by Shi et al. [6], Yang et al. [7], Clouteau and Degrande [8] using three dimensions model. In the latter studies the moving load is equivalently reduced to an immobile dynamic load on the pavement and three dimension model for tunnel with foundation has not been considered.

This paper is devoted to study dynamic response of tunnel and foundation in three dimension model subjected to moving vehicle loads. First, the governing equations are derived by using the finite element procedure. Then, the system's dynamic response is computed by using the Newmark's method and MATLAB program. Finally, an experimental test on the reinforced concrete double tunnel in the Lang-Hoa Lac highway was carried out to validate the numerical model and results.

2. FINITE ELEMENT FORMULATION AND THE GOVERNING EQUATIONS

Consider a double tunnel with pavement-partition wall-arc of arch surrounded by foundation subjected to moving loads along the longitudinal direction of tunnel (Fig. 1). Objective is to determine the dynamic responses of the tunnel skin by finite element method. For finite element model formulation the following assumptions are made: Materials of the system are linear-elastic; load and pavement are not speared in the activity duration of system; tunnel skin and foundation simultaneously work; bindings are absolute and systems work in space model.

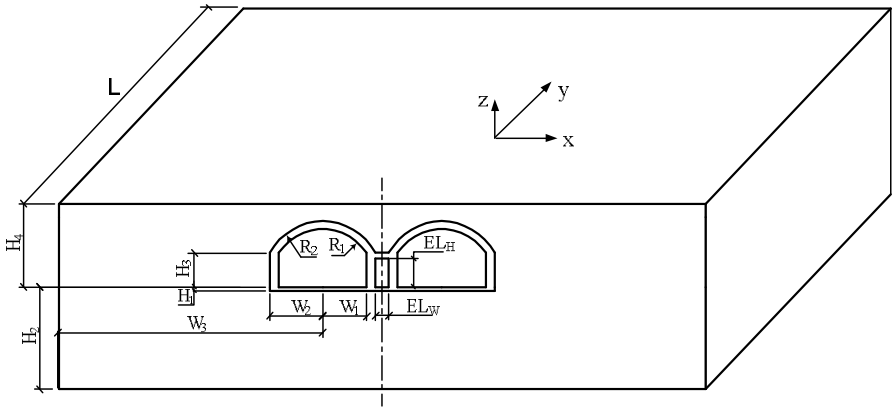

Fig. 1. Model of tunel-foundation system

2.1. Finite element model of tunnel-foundation system

2.1.1. *Elements for pavement and partition wall*

Pavement plate and partition wall (arch tunnel case) or pavement plate, partition wall and tunnel roof (case of tunnel having not arch) are described by bending rectangular four-node elements (Fig. 2). Arbitrary point in the element has positions (x, y) in global coordinate and positions (r, s) in local coordinate [9]. Assume that the thickness of plate element h is a constant and the conditions of Reissner-Mindlin plate theory are satisfied.

In that case displacements u, v and w at an any point (x, y, z) along x, y and z directions [9,10] are defined as

$$\begin{aligned} u(x,y,z,t) &= u_0(x,y,t) + z\theta_y(x,y,t), \\ v(x,y,z,t) &= v_0(x,y,t) - z\theta_x(x,y,t), \\ w(x,y,z,t) &= w_0(x,y,t), \end{aligned} \tag{1}$$

where u_0, v_0, w_0 are the displacements of midplane and θ_x, θ_y - rotations of normal about the y and x axes, respectively. The strain vector is presented in the form

$$\{\varepsilon_p\} = \left\{\{\varepsilon_x \quad \varepsilon_y \quad \gamma_{xy}\} \quad \{\gamma_{xz} \quad \gamma_{yz}\}\right\}^T = \left\{\{\varepsilon^b\}^T \quad \{\varepsilon^s\}^T\right\}^T, \tag{2}$$

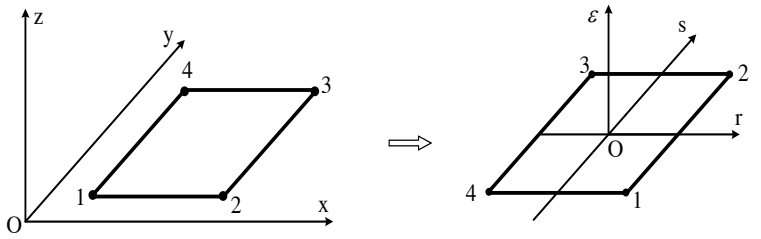

a) Global coordinate b) Local coordinate

Fig. 2. Global and local coordinates of 4-node element

where

$$\left\{\varepsilon^b\right\} = \left\{\frac{\partial u_0}{\partial x} \quad \frac{\partial v_0}{\partial y} \quad \left(\frac{\partial u_0}{\partial y} + \frac{\partial v_0}{\partial x}\right)\right\}^T + z\left\{\frac{\partial \theta_y}{\partial x} \quad -\frac{\partial \theta_x}{\partial y} \quad \left(\frac{\partial \theta_y}{\partial x} - \frac{\partial \theta_x}{\partial y}\right)\right\}^T = \{\varepsilon_0\} + z\{\kappa\}, \tag{3}$$

$$\begin{aligned} \{\varepsilon^s\} &= \left\{\gamma_{xz} \quad \gamma_{yz}\right\}^T = \left\{\frac{\partial w_0}{\partial x} + \theta_y \quad \frac{\partial w_0}{\partial y} - \theta_x\right\}^T, \\ \{\kappa\} &= \left\{\begin{array}{ccc} k_x & k_y & k_{xy}\end{array}\right\}^T = \left\{\frac{\partial \theta_y}{\partial x} \quad -\frac{\partial \theta_x}{\partial y} \quad \left(\frac{\partial \theta_y}{\partial x} - \frac{\partial \theta_x}{\partial y}\right)\right\}^T. \end{aligned} \tag{4}$$

The constitutive equation can be written as

$$\underbrace{\{\sigma\}}_{5\times 1} = \left\{\begin{array}{c} \underbrace{\left\{\sigma^b\right\}}_{3\times 1} \\ \underbrace{\left\{\sigma^s\right\}}_{2\times 1} \end{array}\right\} = \left[\begin{array}{cc} \underbrace{\left[D^b\right]}_{3\times 3} & \underbrace{[0]}_{3\times 2} \\ \underbrace{[0]}_{2\times 3} & \underbrace{[D^s]}_{2\times 2} \end{array}\right] \left\{\begin{array}{c} \underbrace{\left\{\varepsilon^b\right\}}_{3\times 1} \\ \underbrace{\left\{\gamma^s\right\}}_{2\times 1} \end{array}\right\}, \tag{5}$$

where $\left\{\sigma^b\right\}$ is stress vector without shear deformation

$$\left\{\sigma^b\right\} = \begin{Bmatrix}\sigma_x \\ \sigma_y \\ \tau_{xy}\end{Bmatrix} = \frac{E}{1-\nu^2}\begin{bmatrix}1 & \nu & 0 \\ \nu & 1 & 0 \\ 0 & 0 & \dfrac{1-\nu}{2}\end{bmatrix}\begin{Bmatrix}\varepsilon_x \\ \varepsilon_y \\ \gamma_{xy}\end{Bmatrix} = \left[D^b\right]\left\{\varepsilon^b\right\} = \left[D^b\right](\{\varepsilon_0\} + z\{\kappa\}), \tag{6}$$

$\{\sigma^s\}$ is stress vector of shear stress

$$\{\sigma^s\} = \begin{Bmatrix}\tau_{xz} \\ \tau_{yz}\end{Bmatrix} = G\begin{Bmatrix}\gamma_{xz} \\ \gamma_{yz}\end{Bmatrix} = \frac{E}{2(1+\nu)}\begin{bmatrix}1 & 0 \\ 0 & 1\end{bmatrix}\begin{Bmatrix}\gamma_{xz} \\ \gamma_{yz}\end{Bmatrix} = [D^s]\{\varepsilon^s\}, \tag{7}$$

with E is elastic modulus of longitudinal deformation, ν is Poisson ratio.

Using Eqs. (6), (7) the internal force vector $\left\{\sigma^{\text{if}}\right\} = \left\{M_x \quad M_y \quad M_{xy} \quad Q_x \quad Q_y\right\}^T$ can be calculated as

$$\left\{M_x \quad M_y \quad M_{xy}\right\}^T = \int\limits_{-\frac{h}{2}}^{\frac{h}{2}} z \begin{Bmatrix} \sigma_x \\ \sigma_y \\ \tau_{xy} \end{Bmatrix} \mathrm{d}z = \left[D^b\right] \int\limits_{-\frac{h}{2}}^{\frac{h}{2}} z\left(\{\varepsilon_0\} + z\{\kappa\}\right) \mathrm{d}z = \frac{h^3}{12}\left[D^b\right]\{\kappa\},$$

$$\left\{Q_x \quad Q_y\right\}^T = \int\limits_{-\frac{h}{2}}^{\frac{h}{2}} \left[D^s\right]\left\{\varepsilon^s\right\} \mathrm{d}z = \alpha h \left[D^s\right]\left\{\varepsilon^s\right\}.$$

So that one obtains

$$\left\{\sigma^{\text{if}}\right\} = \left[D^{cs}\right]\left\{\varepsilon^{cs}\right\}, \tag{8}$$

where $\left[D^{cs}\right] = \begin{bmatrix} \frac{h^3}{12}\left[D^b\right] & [0] \\ [0] & \alpha h\left[D^s\right] \end{bmatrix}$ - strain matrix, $\left\{\varepsilon^{cs}\right\} = \left\{k_x \quad k_y \quad k_{xy} \quad \gamma_{xz} \quad \gamma_{yz}\right\}^T$ is the vector of curvatures and shear strains, α is the shear strain correction factor, usually $\alpha = 5/6$.

Accordingly to the FEM procedure, the displacements of a point of element are represented as

$$w = \sum_{i=1}^{4} N_i w_i, \quad \theta_x = \sum_{i=1}^{4} N_i \theta_{xi}, \quad \theta_y = \sum_{i=1}^{4} N_i \theta_{yi}, \tag{9}$$

where w_i, θ_{xi}, θ_{yi} are displacements of w, θ_x, θ_y at i^{th} node, respectively, N_i are shape functions. One has

$$\underbrace{\left\{\varepsilon^{cs}\right\}_e}_{5\times 1} = \underbrace{[B]_e}_{5\times 12}\underbrace{\{q\}_e}_{12\times 1} = \sum_{i=1}^{4} \underbrace{[B_i]}_{5\times 3}\underbrace{\{q_i\}}_{3\times 1}. \tag{10}$$

where $[B]_e$ is matrix for internal force determination, $\underbrace{\{q\}_e}_{12\times 1} = \left\{\{q_1\}^T \ \{q_2\}^T \ \{q_3\}^T \ \{q_4\}^T\right\}_e^T$ is vector of node displacement, with $\{q_i\} = \left\{w_i \quad \theta_{xi} \quad \theta_{yi}\right\}^T (i = 1, 2, 3, 4)$.

Substituting (10) into (8) leads to

$$\underbrace{\left\{\sigma^{\text{if}}\right\}}_{5\times 1} = \sum_{i=1}^{4} \underbrace{\left[D^{cs}B_i\right]}_{5\times 3}\underbrace{\{q_i\}}_{3\times 1}, \tag{11}$$

where

$$\left[D^{cs}B_i\right] = \left[D^{cs}B_i\right]^b + \left[D^{cs}B_i\right]^s, \tag{12}$$

$\left[D^{cs}B_i\right]^b$, $\left[D^{cs}B_i\right]^s$ are matrices corresponding to bending moment and shear force, respectively [9].

Using (10), (11) now we can calculate the total potential energy [9,11] as

$$\Pi_e = \frac{1}{2}\int\limits_{A_e} \left\{\sigma^{\text{if}}\right\}_e^T [D^{cs}] \left\{\sigma^{\text{if}}\right\}_e \mathrm{d}A_e - \int\limits_{A_e} wp\,\mathrm{d}A_e = \frac{1}{2}\{q\}_e^T [K^p]_e \{q\}_e - \{q\}_e^T \{P\}_e, \quad (13)$$

with

$$\begin{aligned} \underbrace{[K^p]_e}_{12\times 12} &= \int\limits_{A_e} [B]^T [D^{cs}] [B]\ \mathrm{d}A_e, \\ \underbrace{\{P\}_e}_{12\times 1} &= \int\limits_{A_e} [N]^T p\,\mathrm{d}A_e, \end{aligned} \quad (14)$$

are stiffness matrix and node loading vector of the element, respectively, $\underbrace{[N]}_{1\times 12} = \begin{bmatrix} N_1 & 0 & 0 & N_2 & 0 & 0 & N_3 & 0 & 0 & N_4 & 0 & 0 \end{bmatrix}$, p is pressure of intensity.

Kinetic energy T_e of element is determined by [9,11]

$$T_e = \frac{1}{2}\int\limits_{V_e} \rho \{\dot{u}\}_e^T \{\dot{u}\}_e\ \mathrm{d}V_e \frac{1}{2}\{\dot{q}\}_e^T \left(\int\limits_{V_e} \rho [N]^T [N]\ \mathrm{d}V_e\right) \{\dot{q}\}_e = \frac{1}{2}\{\dot{q}\}_e^T [M]_e \{\dot{q}\}_e, \quad (15)$$

where ρ-mass density, $\{\dot{q}\}_e$-velocity vector, and

$$[M^p]_e = \int\limits_{V_e} \rho [N]^T [N]\ \mathrm{d}V_e. \quad (16)$$

2.1.2. *Elements for arc of arch*

Suppose that arc of arch is a shallow cylindrical shell that can be described by 4 nodes flat shell elements with 6 degrees of freedom $u_i, v_i, w_i, \theta_{xi}, \theta_{yi}, \theta_{zi}$ per node and vector of element node displacement

$$\left\{q^{sh}\right\}_e = \left\{ \{q^p\}_e^T \quad \{q^f\}_e^T \quad \{q^\theta\}_e^T \right\}^T, \quad (17)$$

where $\underbrace{\{q^p\}_e}_{12\times 1} = \{w_1 \quad \theta_{x1} \quad \theta_{y1} \quad w_2 \quad \theta_{x2} \quad \theta_{y2} \quad \ldots \quad w_4 \quad \theta_{x4} \quad \theta_{y4}\}^T$-vector of node displacement of bending plate element, $\{q^f\}_e = \{u_1 \quad v_1 \quad u_2 \quad v_2 \quad u_3 \quad v_3 \quad u_4 \quad v_4\}^T$-vector of node displacement of tension or compression plate element $\{q^\theta\}_e = \{\theta_{z1} \quad \theta_{z2} \quad \theta_{z3} \quad \theta_{z4}\}^T$ -vector of node twist surrounded the axis z of elements.

Following [9, 12] the matrix of flat shell element stiffness can be derived as

$$\underbrace{\left[K^{sh}\right]_e}_{24\times24} = \begin{bmatrix} \underbrace{[K^p]_e}_{12\times12} & \underbrace{[0]}_{12\times8} & \underbrace{[0]}_{12\times4} \\ \underbrace{[0]}_{8\times12} & \underbrace{\left[K^f\right]_e}_{8\times8} & \underbrace{[0]}_{8\times4} \\ \underbrace{[0]}_{4\times12} & \underbrace{[0]}_{4\times8} & \underbrace{[K^{rz}]_e}_{4\times4} \end{bmatrix}, \tag{18}$$

where: $[K^p]_e$-stiffness matrix of bending plate element, $\left[K^f\right]_e$-stiffness matrix of tension or compression plate element [9] and $[K^{rz}]_e$-stiffness matrix of twist plate element. In fact, the components $k_{rz}(i,j)$ of matrix $[K^{rz}]_e$ are equal to zero (in the calculation these components are considered to be very small, namely $k_{rz}(i,j) = 10^{-3} \times \max(k_{(m,n)})$, where $k_{(m,n)}$ are components of matrices $[K^p]_e$ and $\left[K^f\right]_e$ [9, 12]).

Similarly, mass matrix of flat shell element [9, 12] is

$$\underbrace{\left[M^{sh}\right]_e}_{24\times24} = \begin{bmatrix} \underbrace{[M^p]_e}_{12\times12} & \underbrace{[0]}_{12\times8} & \underbrace{[0]}_{12\times4} \\ \underbrace{[0]}_{8\times12} & \underbrace{\left[M^f\right]_e}_{8\times8} & \underbrace{[0]}_{8\times4} \\ \underbrace{[0]}_{4\times12} & \underbrace{[0]}_{4\times8} & \underbrace{[M^{rz}]_e}_{4\times4} \end{bmatrix}. \tag{19}$$

Load vector, stiffness matrix and mass matrix of element shell in the global coordinate system are determined as follow [12]

$$\left\{q^{sh}\right\}_e^g = \left[T^{sh}\right]^T \left\{q^{sh}\right\}_e, \left[K^{sh}\right]_e^g = \left[T^{sh}\right]^T \left[K^{sh}\right]_e \left[T^{sh}\right], \left[M^{sh}\right]_e^g = \left[T^{sh}\right]^T \left[M^{sh}\right]_e \left[T^{sh}\right], \tag{20}$$

where $\underbrace{\left[T^{sh}\right]}_{24\times24}$ is transformation coordinate system matrix.

2.1.3. *Elements for foundation layers*

For foundation layers, using the hexagonal 8-node element with 3 degrees of freedom of each node one can obtain the following relationship

$$\{\varepsilon\}_e = [B]\{q\}_e \tag{21}$$

for strain vector $\{\varepsilon\}_e$ at a point of element and node displacement $\{q\}_e$ [9, 12]. In the above equation the notations are introduced

$$\{\varepsilon\}_e = \begin{Bmatrix} \varepsilon_x & \varepsilon_y & \varepsilon_z & \gamma_{xy} & \gamma_{yz} & \gamma_{zx} \end{Bmatrix}^T, [B] = [\partial][N] = \begin{bmatrix} [B_1] & [B_2] & [B_3] & ... & [B_8] \end{bmatrix},$$

$[N]$ is mode shape function matrix of element. Therefore, the stiffness matrix of element is [12]

$$[K]_e = \int_{V_e} [B]^T [D] [B] \, \mathrm{d}V_e, \tag{22}$$

with $[D]$ is element material matrix. The mass load vector is determined by [12]

$$\{P\}_e = \int_{V_e} [N]^T \{g\} \, \mathrm{d}V = \int_{V_e} [N]^T \left\{ \begin{array}{ccc} g_x & g_y & g_z \end{array} \right\}^T \mathrm{d}V, \tag{23}$$

2.2. Modeling of vehicle movement on pavement plate

Let's consider a four wheel vehicle modeled by 4-degree-of-freedom system which moves on the pavement plate with the trajectory $x = x(t), y = y(t)$ and velocity $\vec{v} = \vec{v}(t)$ (see Fig. 3). The mass of vehicle body m is derived as absolute solid body and pavement plate is springs with stiffness $k_{f1}, k_{f2}, k_{r1}, k_{r2}$ and damping elements c_f, c_r, respectively (Fig. 4b, c). The inertia moment of vehicle body with center-of-mass G is J. The distances from G to the front axle and rear axle are l_f and l_r, respectively. The position of vehicle body is determined by parameters: vertical displacement u of center-of-mass G, rotation displacement in plane xz, vertical displacement z_f of front wheels, vertical displacement z_r of rear wheels. The considered system is 4-degree-of-freedom system [13]. Assumes that vibration amplitude is small, vehicle body is in initial horizontal direction.

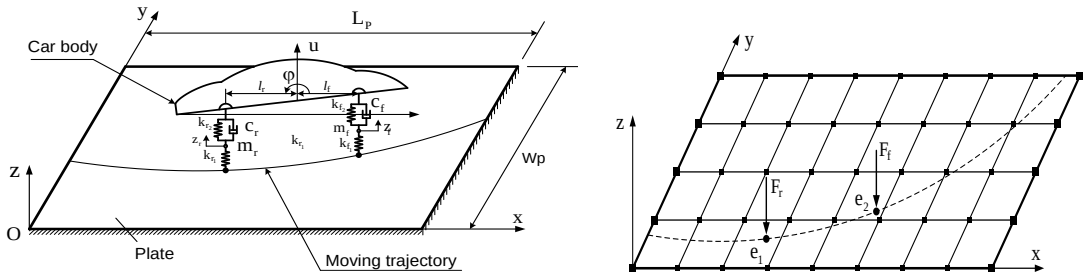

(a) Real model (b) FEM model

Fig. 3. Plate subjected to 4-degree-of-freedom vehicle load model

At a time, the vehicle body is subjected to gravity force $P = mg$, exiting forces F_r, F_f, and inertia forces $m\ddot{u}, J\ddot{\varphi}$ (Fig. 4a).

The equilibrium equation system of vehicle body is written as follows

$$\begin{array}{l} m\ddot{u} + F_r + F_f + mg = 0, \\ J\ddot{\varphi} - F_r l_r + F_f l_f = 0. \end{array} \tag{24}$$

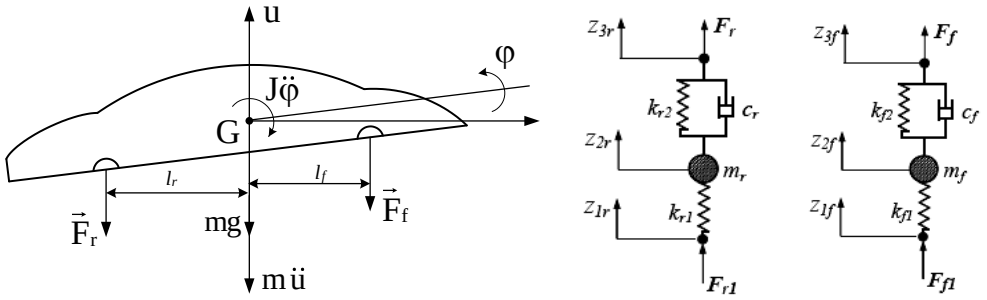

(a) Vehicle body (b) Wheel system, front suspension (c) Wheel system, rear suspension

Fig. 4. Applied forces of vehicle

where $\ddot{u}$ is vertical acceleration, $\ddot{\varphi}$ is angular acceleration in the plane xz of vehicle body. The equilibrium equations for wheels and suspension are

$$\begin{aligned} &k_{r1}\left(z_{1r}-z_{2r}\right)=F_{r1},\\ &m_r\ddot{z}_{2r}+c_r\left(\dot{z}_{2r}-\dot{u}+\dot{\varphi}l_r\right)-k_{r1}\left(z_{1r}-z_{2r}\right)+k_{r2}\left(z_{2r}-u+\varphi l_r\right)=0,\\ &c_r\left(\dot{u}-\dot{z}_{2r}-\dot{\varphi}l_r\right)+k_{r2}\left(u-z_{2r}-\varphi l_r-\delta_{2r}\right)=F_r. \end{aligned} \tag{25}$$

$$\begin{aligned} &k_{f1}\left(z_{1f}-z_{2f}\right)=F_{f1},\\ &m_f\ddot{z}_{2f}+c_f\left(\dot{z}_{2f}-\dot{u}+\dot{\varphi}l_f\right)-k_{f1}\left(z_{1f}-z_{2f}\right)+k_{f2}\left(z_{2f}-u+\varphi l_f\right)=0,\\ &c_f\left(\dot{u}-\dot{z}_{2f}+\dot{\varphi}l_f\right)+k_{f2}\left(u-z_{2f}+\varphi l_f-\delta_{2f}\right)=F_f. \end{aligned} \tag{26}$$

where δ_{2r} is static deformation of spring with stiffness k_{r2} and δ_{2f} is static deformation of spring with stiffness k_{f2}.

Combining (24), (25) and (26) leads to the differential equations for vibration of the systems (4-degree-of-freedom vehicle)

$$\begin{aligned} &m\ddot{u}+c_r(\dot{u}-\dot{z}_{2r}-\dot{\varphi}l_r)+c_f\left(\dot{u}-\dot{z}_{2f}+\dot{\varphi}l_f\right)+k_{r2}(u-z_{2r}-\varphi l_r)+k_{f2}\left(u-z_{2f}+\varphi l_f\right)=0,\\ &J\ddot{\varphi}-l_rc_r(\dot{u}-\dot{z}_{2r}-\dot{\varphi}l_r)+l_fc_f\left(\dot{u}-\dot{z}_{2f}+\dot{\varphi}l_f\right)-l_rk_{r2}(u-z_{2r}-\varphi l_r)+l_fk_{f2}\left(u-z_{2f}+\varphi l_f\right)=0,\\ &m_r\ddot{z}_{2r}-c_r\left(\dot{u}-\dot{z}_{2r}-\dot{\varphi}l_r\right)+k_{r1}\left(z_{2r}-z_{1r}\right)-k_{r2}\left(u-z_{2r}-\varphi l_r\right)=0,\\ &m_f\ddot{z}_{2f}-c_f\left(\dot{u}-\dot{z}_{2f}+\dot{\varphi}l_f\right)+k_{f1}\left(z_{2f}-z_{1f}\right)-k_{f2}\left(u-z_{2f}+\varphi l_f\right)=0, \end{aligned} \tag{27}$$

where z_{1r}, z_{1f} are vertical displacements of pavement plate at position of contact with the wheels and z_{2r}, z_{2f} are displacements of mass m_r and m_f, respectively.

Let (ξ_1, η_1) and (ξ_2, η_2) be coordinates of the contact points where loads F_{r1} and F_{r2} are applied to elements e_1 and e_2 of pavement plate. The global coordinate systems of the plate elements are $(x_1 = x_{01} + \xi_1, y_1 = y_{01} + \eta_1)$ and $(x_2 = x_{02} + \xi_2, y_2 = y_{02} + \eta_2)$. Using the representation (9) for flexural displacement we obtain

$$\begin{aligned} z_{1r}&=\left[N^{e_1}\left(\xi_1,\eta_1\right)\right]\left\{q^{e_1}\right\}=\left[N\left(\xi_1,\eta_1\right)\right]\left[G\right]^{-1}\left\{q^{e_1}\right\},\\ z_{1f}&=\left[N^{e_2}\left(\xi_2,\eta_2\right)\right]\left\{q^{e_2}\right\}=\left[N\left(\xi_2,\eta_2\right)\right]\left[G\right]^{-1}\left\{q^{e_2}\right\}, \end{aligned} \tag{28}$$

where $\underbrace{[G]}_{12\times12}$ is matrix of geometrical properties for the elements [9]. Substituting (28) into (27), leads to the equation

$$[M^v]\{\ddot{q}^v\} + [C^v]\{\dot{q}^v\} + [K^v]\{q^v\} = \{F^v\}, \tag{29}$$

where vectors of acceleration, velocity and displacement $\{\ddot{q}^v\}$, $\{\dot{q}^v\}$, $\{q^v\}$; matrices of mass, damping and stiffness $[M^v]$, $[C^v]$, $[K^v]$ and load vector $\{F^v\}$ are determined, respectively, as

$$\{q^v\} = \begin{Bmatrix} u & \varphi & z_{2r} & z_{2f} \end{Bmatrix}^T, \quad [M^v] = \begin{bmatrix} m & 0 & 0 & 0 \\ 0 & J & 0 & 0 \\ 0 & 0 & m_r & 0 \\ 0 & 0 & 0 & m_f \end{bmatrix}, \tag{30}$$

$$[C^v] = \begin{bmatrix} c_r + c_f & l_f c_f - l_r c_r & -c_r & -c_f \\ l_f c_f - l_r c_r & l_r^2 c_r + l_f^2 c_f & l_r c_r & -l_f c_f \\ -c_r & l_r c_r & c_r & 0 \\ -c_f & -l_f c_f & 0 & c_f \end{bmatrix}, \{F^v\} = \begin{Bmatrix} 0 \\ 0 \\ k_{1r}\left[N\left(\xi_1,\eta_1\right)\right][G]^{-1}\{q^{e_1}\} \\ k_{1f}\left[N\left(\xi_2,\eta_2\right)\right][G]^{-1}\{q^{e_2}\} \end{Bmatrix}, \tag{31}$$

$$[K^v] = \begin{bmatrix} k_{r2} + k_{f2} & l_f k_{f2} - l_r k_{r2} & -k_{r2} & -k_{f2} \\ l_f k_{f2} - l_r k_{r2} & l_r^2 k_{r2} + l_f^2 k_{f2} & l_r k_{r2} & -l_f k_{f2} \\ -k_{r2} & l_r k_{r2} & k_{r1} + k_{r2} & 0 \\ -k_{f2} & -l_f k_{f2} & 0 & k_{f1} + k_{f2} \end{bmatrix}. \tag{32}$$

Assuming that the plate element e_1 is subjected to moving load F_{r1} and element e_2 subjected to moving load F_{f1}, the forces can be rewritten as

$$\begin{aligned} F_{r1} &= k_{r1}\left(z_{1r} - z_{2r}\right) = m_r \ddot{z}_{2r} - c_r\left(\dot{u} - \dot{z}_{2r} - \dot{\varphi} l_r\right) - k_{r2}\left(u - z_{2r} - \varphi l_r\right), \\ F_{f1} &= k_{f1}\left(z_{1f} - z_{2f}\right) = m_f \ddot{z}_{2f} - c_f\left(\dot{u} - \dot{z}_{2f} + \dot{\varphi} l_f\right) - k_{f2}\left(u - z_{2f} + \varphi l_f\right). \end{aligned} \tag{33}$$

By using Delta-Dirac function $\delta(\cdot)$ [9, 11, 14] the concentrated loads (33) can be represented as the distribution force $p_i(\xi,\eta,t)$ as follows

$$\begin{aligned} p_{r1}\left(\xi,\eta,t\right) &= F_{r1}\cdot\delta\left(\xi - \xi_1\right)\cdot\delta\left(\eta - \eta_1\right), \\ p_{f1}\left(\xi,\eta,t\right) &= F_{f1}\cdot\delta\left(\xi - \xi_2\right)\cdot\delta\left(\eta - \eta_2\right). \end{aligned} \tag{34}$$

Therefore, the node load vector of element becomes [9]

$$\{F^{e_1}\} = \left[N\left(\xi_1,\eta_1\right)\right]^T F_{r1}, \quad \{F^{e_2}\} = \left[N\left(\xi_2,\eta_2\right)\right]^T F_{f1}. \tag{35}$$

Substituting (33) into (35), leads to

$$\begin{aligned} \left\{F^{e1}\right\} &= \left[M^{1r}\right]\{\ddot{q}^v\} + \left[C^{1r}\right]\{\dot{q}^v\} + \left[K^{1r}\right]\{q^v\}, \\ \left\{F^{e2}\right\} &= \left[M^{1f}\right]\{\ddot{q}^v\} + \left[C^{1f}\right]\{\dot{q}^v\} + \left[K^{1f}\right]\{q^v\}, \end{aligned} \tag{36}$$

where

$$\left[M^{1r}\right] = \left[0 \quad 0 \quad \left[N\left(\xi_1,\eta_1\right)\right]^T m_r \quad 0\right], \quad \left[M^{1f}\right] = \left[0 \quad 0 \quad 0 \quad \left[N\left(\xi_2,\eta_2\right)\right]^T m_f\right],$$
$$\left[C^{1r}\right] = \left[-\left[N\left(\xi_1,\eta_1\right)\right]^T c_r \quad \left[N\left(\xi_1,\eta_1\right)\right]^T c_r l_r \quad \left[N\left(\xi_1,\eta_1\right)\right]^T c_r \quad 0 \right],$$
$$\left[C^{1f}\right] = \left[-\left[N\left(\xi_2,\eta_2\right)\right]^T c_f \quad -\left[N\left(\xi_2,\eta_2\right)\right]^T c_f l_f \quad 0 \quad \left[N\left(\xi_2,\eta_2\right)\right]^T c_f \right],$$
$$\left[K^{1r}\right] = \left[-\left[N\left(\xi_1,\eta_1\right)\right]^T k_{r2} \quad \left[N\left(\xi_1,\eta_1\right)\right]^T k_{r2} l_r \quad \left[N\left(\xi_1,\eta_1\right)\right]^T k_{r2} \quad 0 \right],$$
$$\left[K^{1f}\right] = \left[-\left[N\left(\xi_2,\eta_2\right)\right]^T k_{f2} \quad -\left[N\left(\xi_2,\eta_2\right)\right]^T k_{f2} l_f \quad 0 \quad \left[N\left(\xi_2,\eta_2\right)\right]^T k_{f2} \right].$$

So, the equations of motion for elements e_1 and e_2 get to be

$$\left[M^{e_1}\right]\left\{\ddot{q}^{e_1}\right\} + \left[C^{e_1}\right]\left\{\dot{q}^{e_1}\right\} + \left[K^{e_1}\right]\left\{q^{e_1}\right\} = \left\{F^{e_1}\right\}, \tag{37}$$
$$\left[M^{e_2}\right]\left\{\ddot{q}^{e_2}\right\} + \left[C^{e_2}\right]\left\{\dot{q}^{e_2}\right\} + \left[K^{e_2}\right]\left\{q^{e_2}\right\} = \left\{F^{e_2}\right\}, \tag{38}$$

with $\left[M^{e_i}\right], \left[C^{e_i}\right], \left[K^{e_i}\right], (i = 1,2)$ are matrices of mass, damping and stiffness, respectively.

Introducing the node displacement vector

$$\left\{q^e\right\}_v = \left\{\left\{q^{e_1}\right\}^T \quad \left\{q^{e_2}\right\}^T \quad \left\{q^v\right\}^T\right\}^T, \tag{39}$$

composed off those of the plate elements e_1, e_2 and body car and combining Eqs. (36) (37), (38) with (29) allow the equations of motion for vehicle system and pavement elements to be written in the matrix form

$$\left[M^e\right]_v \left\{\ddot{q}^e\right\}_v + \left[C^e\right]_v \left\{\dot{q}^e\right\}_v + \left[K^e\right]_v \left\{q^e\right\}_v = \left\{F^e\right\}_v, \tag{40}$$

with

$$\left[M^e\right]_v = \begin{bmatrix} \left[M^{e1}\right] & [0] & -\left[M^{1r}\right] \\ [0] & \left[M^{e2}\right] & -\left[M^{1f}\right] \\ [0] & [0] & \left[M^v\right] \end{bmatrix} = \left[M_t^e\right] + \left[M_p^e\right]_v,$$
$$\left[K^e\right]_v = \begin{bmatrix} \left[K^{e1}\right] & [0] & -\left[K^{1r}\right] \\ [0] & \left[K^{e2}\right] & -\left[K^{1f}\right] \\ [0] & [0] & \left[K^v\right] \end{bmatrix} = \left[K_t^e\right] + \left[K_p^e\right]_v,$$
$$\left[C^e\right]_v = \begin{bmatrix} \left[C^{e1}\right] & [0] & -\left[C^{1r}\right] \\ [0] & \left[C^{e2}\right] & -\left[C^{1f}\right] \\ [0] & [0] & \left[C^v\right] \end{bmatrix} = \left[C_t^e\right] + \left[C_p^e\right]_v, \quad \left\{F^e\right\}_v = \begin{Bmatrix} \{0\} \\ \{0\} \\ \left\{F^v\right\} \end{Bmatrix}.$$

Assembling all elements matrices and nodal force vectors the governing equations of motions of the total system can be derived as

$$[M]\{\ddot{q}\} + [C]\{\dot{q}\} + [K]\{q\} = \{F\}, \tag{41}$$

with

$$[M] = \sum_e \left[M_t^e\right] + \sum_e \left[M_p^e\right]_v, \quad [K] = \sum_e \left[K_t^e\right] + \sum_e \left[K_p^e\right]_v,$$
$$[C] = \sum_e \left[C_t^e\right] + \sum_e \left[C_p^e\right]_v, \quad \{F\} = \sum_e \left\{F^e\right\}_v,$$

This is a linear differential equation system with time dependence coefficient that can be solved by using direct integration Newmark's method. A Matlab program named by 3D_Structures_Moving_2014 was conducted to solve equation (41).

3. NUMERICAL ANALYSIS

3.1. Validation of computer program

To validate the present approach, consider a tunnel with square box cross section area $H_{tun} \times W_{tun} = 4\,\text{m} \times 4\,\text{m}$, thickness of wall $t_{tun} = 0,5\,\text{m}$, length $L_{tun} = 10\,\text{m}$ in the homogeneous foundation, depth from center of tunnel section to freely surface of foundation is $h_{tun} = 4\,\text{m}$, subjected by concentric loading at the center point of pavement, load law $P(t) = P_0 \sin 2\pi f t$, with P_0 = 50000 N, $f = 10\,\text{Hz}$. Tunnel is made by concrete with elastic modulus $\text{E}_{tun} = 0.34 \times 10^7\,\text{N/cm}^2$, Poisson ratio ν_{tun} = 0.3, mass density $\rho_{tun} = 2.5 \times 10^{-3}\,\text{kg/cm}^3$; characteristic of foundation: elastic modulus $E_f = 0.2 \times 10^6\,\text{N/cm}^2$, Poisson ratio ν_f = 0.35, mass density $\rho_f = 1.8 \times 10^{-3}\,\text{kg/cm}^3$. The considered region dimensions: $H_s \times W_s \times L_s = 20\,\text{m} \times 40\,\text{m} \times 10\,\text{m}$. The results are obtained by using 3D_Structures_Moving_2014 and Ansys 13.0 programs. The first three of fundamental frequency and displacement amplitude at loaded point for two methods are shown in Tab. 1.

Table 1. Comparison between present results with Ansys software results

		Fundamental frequency			Maximum displacement
Characteristics		f_1[Hz]	f_2[Hz]	f_3[Hz]	$W_{\max}$[cm]
Method	Ansys 13.0	36.21	98.36	142.84	0.268
	Present	36.54	98.69	143.18	0.271
Different (%)		0.91	0.34	0.25	1.12

This comparison shows that the good agreements are obtained, the difference is very small ($\leq$ 0.25% for fundamental frequency and 1.12% - for displacement).

3.2. Numerical results

A concrete double tunnel with symmetric cross section, as shown in Fig. 5 is considered. The tunnel is subjected to moving load of 4-wheel vehicle which moves in longitudinal direction of the left tunnel with velocity v = 60 km/h. Length of tunnel L = 20 m; wall thickness $t_1 = t_2 = W_2 - W_1$ = 5.95 m – 4.45 m = 1.5 m; wall height H_3 = 3.6 m; pavement thickness H_1 = 0.4 m; tunnel width $2W_1$ = 9.5 m, radius of arch R_1 = 6.5 m, R_2 = 8.5 m, respectively. Dimension of cross section of hollow box (serape 2 single tunnels) $EL_H \times EL_W$ = 3 m×1.5 m. Elastic modulus of concrete $E_c = 3.4 \times 10^{10}$ N/m2; Poisson ratio ν_c = 0.3; mass density ρ_c = 2500 kg/m^3. Accuracy of iteration ε_d = 0.5%, considered region dimensions $H \times W \times L = 20\,\text{m} \times 70\,\text{m} \times 20\,\text{m}$. Three foundation layers 1, 2, 3 with properties are presented in Tab. 2.

Vehicle body mass m = 7000 kg, m_f = 600 kg, m_r = 900 kg, inertia moment of vehicle body about the center-of-mass $J = 30000\,\text{kgm}^2$, distances from front wheel and

Table 2. Foundation properties

Layer	Depth (m)	E_f (N/cm^2)	ν_f	ρ_f (kg/m^3)
1	1.4	0.20×10^6	0.28	1.70×10^3
2	4.2	0.44×10^6	0.25	1.90×10^3
3	18.6	0.90×10^6	0.25	2.15×10^3

rear wheel are $l_f = 3.2\,\text{m}$, $l_r = 1.8\,\text{m}$, respectively, elastic spring stiffness are k_{f1} = 3000000 N/m, k_{f2} = 450000 N/m, k_{r1} = 4000000 N/m, k_{r2} = 700000 N/m, damping coefficients $c_f = c_r = 500\,\text{Ns/m}$. Considered points are A$(-6.7, 10, 10.8)$, the middle of pavement and in the foundation surface. The system model and FEM configuration are shown in Figs. 5-6.

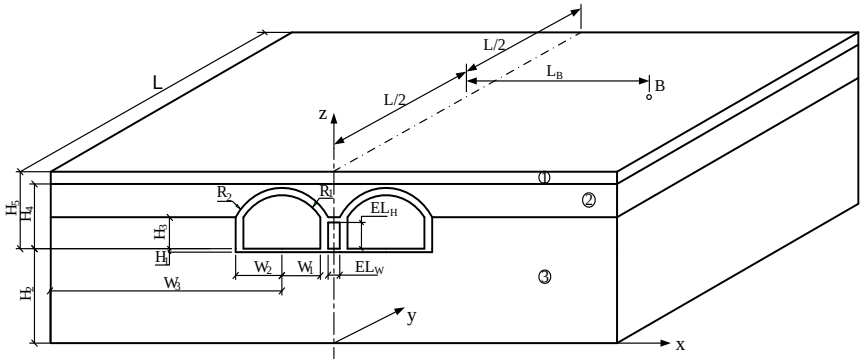

Fig. 5. Model of double tunnel

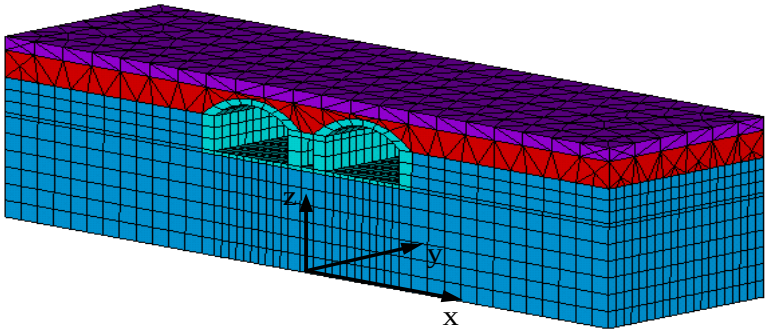

Fig. 6. Configuration of FEM

Fig. 7 shown the relationship of displacement amplitude at point A (z-dir.) and frequency. And we have 4 first natural frequency are $f_1 = 19.82, f_2 = 20.89, f_3 = 21.93, f_4 = 22.16$ (Hz). Displacement and acceleration response results of considered points are shown in Figs. 8-9.

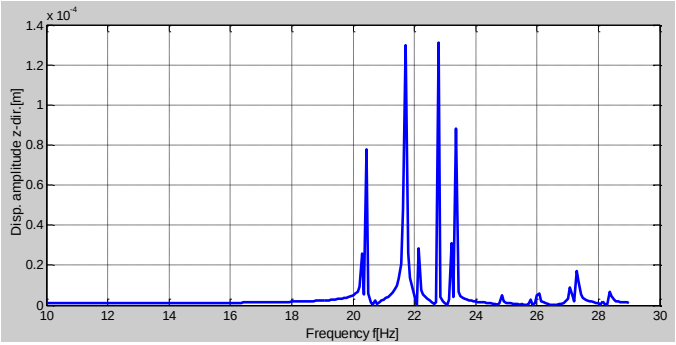

Fig. 7. Vertical displacement amplitudefrequency

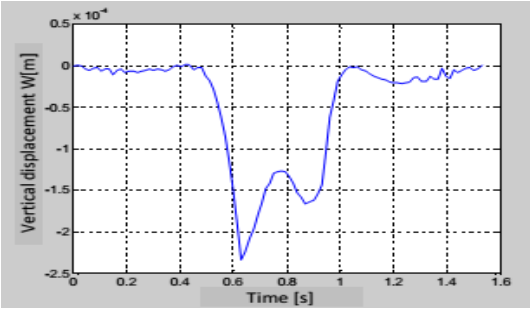

Fig. 8. Vertical displacement response at A

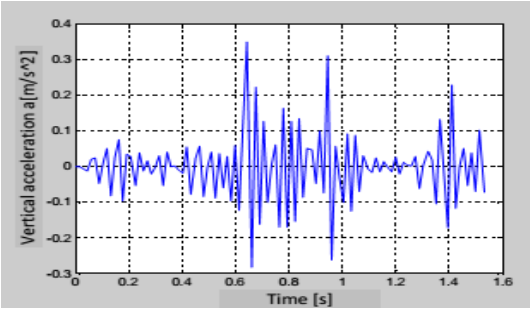

Fig. 9. Vertical acceleration response at A

3.2.1. *Effect of speed of load*

Displacement responses at the point A are shown in Fig. 10 with the speed of vehicle various from 50 km/h to 100 km/h, variation of maximum displacement at point B are presented in Fig. 11.

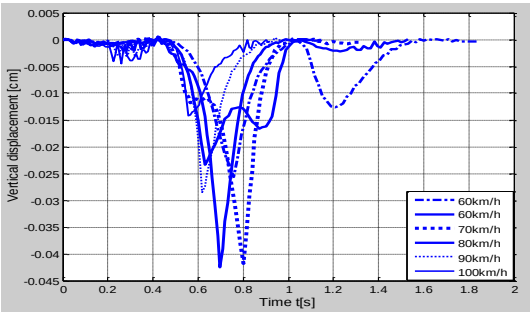

Fig. 10. Vertical displacement response at point A

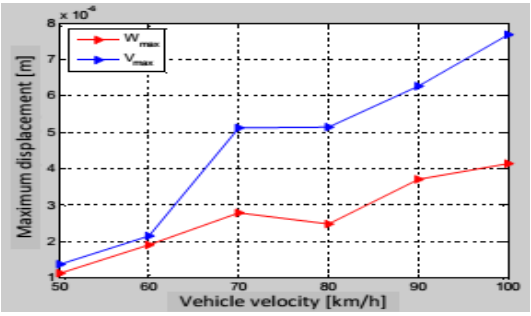

Fig. 11. Variation of maximum displacement at point B

3.2.2. *Effect of foundation surrounding tunnel*

In this section, elastic modulus E_3 of third foundation layer (the foundation surrounds tunnel) varies from $0.2\times10^6\,\mathrm{N/cm^2}$ to $2.0\times10^6\,\mathrm{N/cm^2}$. Obtained dynamic responses are shown in Figs. 12-13.

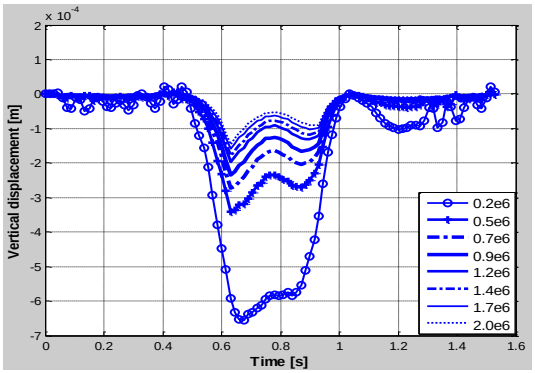

Fig. 12. Vertical displacement response at point A

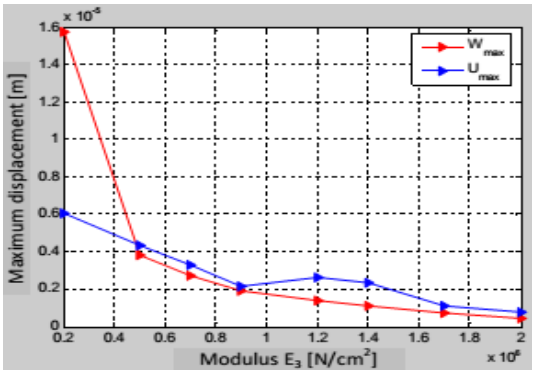

Fig. 13. Maximum displacement at point B

3.2.3. *Effect of tunnel type*

Consider two tunnel types: box-arch section (Type 1) and box section (Type 2) with the same pavement, depth of wall and total section area. Dynamic responses of point A are shown in Figs. 14-15. The result shows that the displacement, acceleration and stress of arc of arch tunnel are smaller than those of flat roof tunnel, and therefore load-carrying capacity of arc of arch tunnel is larger than one of flat roof tunnel.

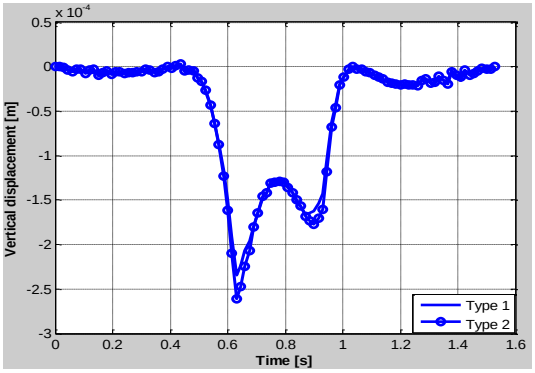

Fig. 14. Vertical displacement responses

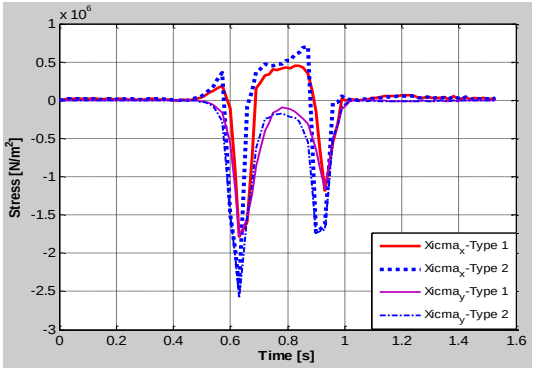

Fig. 15. Stress responses

4. EXPERIMENTAL VALIDATION

4.1. Experimental model and equipment

4.1.1. *Tunnel*

The experiment was carried out for the double tunnel, N° 05-TEDI-003-H at Km7 +358 Lang-Hoa Lac expressway, Hanoi. Its cross section is rectangular box, made by reinforced concrete, (see Fig. 16).

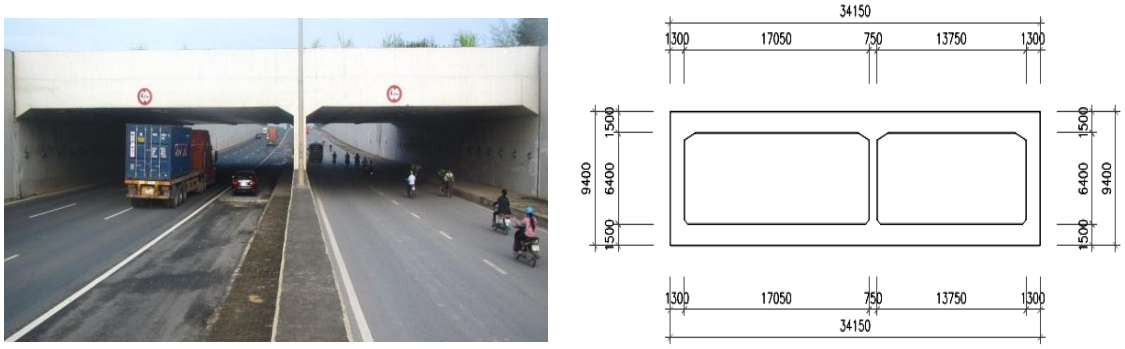

(a) Experimental tunnel (b) Cross section dimension

Fig. 16. Configuration of experimental tunnel

4.1.2. *Loading generation*

Loading is excited by passenger cars of four wheels and conversion parameters: $m = 6600\,\text{kg}$, $m_f = 320\,\text{kg}$, $m_r = 410\,\text{kg}$, $J = 21000\,\text{kgm}^2$, $l_f = 3.2\,\text{m}$, $l_r = 1,8\,\text{m}$, $k_{f1} = 2400000\ \text{N/m}$, $k_{r1} = 3600000\,\text{N/m}$, $k_{f2} = 390000\,\text{N/m}$, $k_{r2} = 540000\,\text{N/m}$, $c_f = c_r = 460\,\text{Ns/m}$.

4.1.3. *Acceleration sensor, resistors plate*

Acceleration sensors ARF-10A are placed on the right of pavement plate to determine vertical acceleration and at the longitudinal tunnel position; resistor plates are attached 1m from acceleration sensor position in longitudinal tunnel to determined relative deformation. Accelerometer specifications are: mass: 2 g, sensitivity: $0.5\,\text{mV}/(\text{m}/\text{s}^2)$, the frequency ranges: 1 to 12000 ($\pm 10\%$) Hz, peak acceleration: $10\,\text{m}/\text{s}^2$, accuracy: $\leq 0.05\%$ (see Figs. 17-18).

4.1.4. *Dynamic measurement system*

Dynamic measurement system SDA-810C (Japan), made in 2010, with: 8 channels, linear frequency response: 10 kHz, electronic source: DC10.5-30V 1.4A; AC170-250V 50/60 Hz 25VA, accuracy: 0.0025%, resolution ADC: 16 bit, sampling rate: 19.2 kHz. This equipment gathers in-situ data that are stored into a computer.

Consider three velocity levels of vehicle 30 km/h, 40 km/h, 50 km/h, surcharge 15 times for each velocity level ($n = 15$).

(a) Experimental equipment preparation (b) Acceleration and deformation sensor disposition

Fig. 17. Experimental preparation

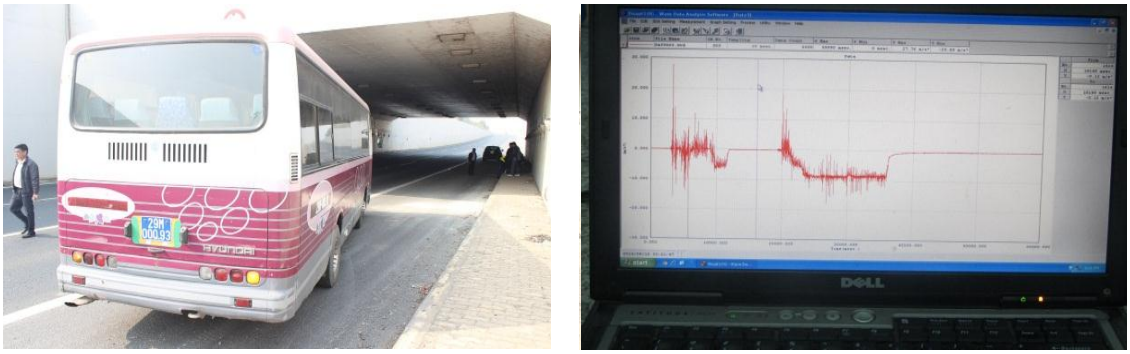

(a) Vehicle (b) Result on the screen (01 time)

Fig. 18. Experimental procedure

4.2. Experimental results

The comparison of results between theoretical calculation by 3D_Structures_ Moving_2014 program and experimental work (with three velocity levels) is presented in Fig. 19 and Tab. 3.

Table 3. Maximum acceleration of considered point

Car velocity V [km/h]		30.0	40.0	50.0
Acceleration a_z[m/s^2]	3D_Structures_Moving_2014 (Theoretical)	0.1947	0.2328	0.2616
	Experimental	0.1746	0.2063	0.2971
Different [%]		11.51	12.85	13.55

It is obtained that the dynamic responses measured at the considered points are more uneven than those by theoretical calculation. The maximum differences of vertical

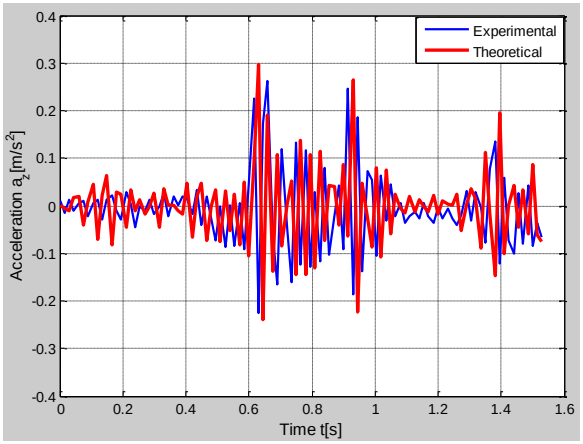

Fig. 19. Vertical acceleration responses at considered point ($V = 50\,\mathrm{km/h}$)

acceleration with three velocity levels are from 11.51% to 13.55%. This result shows that experimental results agree with calculation results. Therefore, we realize that 3D_Structures_Moving_2014 calculation program is reliable.

5. CONCLUSION

This paper presented an algorithm of element finite method established for dynamic analysis of tunnel and foundation in space model subjected to moving loads of vehicle. Numerical investigation has been carried out for an example with different parameters and showed effects of parameters of structure and load to the dynamic response of tunnel-foundation system. The established finite element model and the computer program were tested on a real tunnel. The obtained experimental results are acceptably agreed with the numerical ones.

REFERENCES

[1] S. C. Möller, P. A. Vermeer, and P. G. Bonnier. A fast 3D tunnel analysis. In *Second MIT Conference on Computational Fluid and Solid Mechanics*, (2010), pp. 1–4.

[2] P. G. Bonnier, S. C. Möller, and P. A. Vermeer. Bending moments and normal forces in tunnel linings. In *5th European Conference of Numerical Methods in Geotechnical Engineering, Paris, France*, (2002), pp. 515–522.

[3] H. J. Kim, J. H. Park, and Y. S. Shin. Dynamic analysis of tunnel structures considering soil-structure interaction. *Division of Environmental, Civil and Transportation Engineering, Ajou University, Journal of the KOSOS*, **20**, (1), (2006), pp. 101–106.

[4] A. Sramoon, P. Mruetusatorn, B. Lekhak, and R. Sittipod. Design of reinforced concrete linings of NN2 headrace tunnel. *CEAT Journal*, **3**, (2009), pp. 29–34.

[5] M. F. M. Hussein and H. E. M. Hunt. Dynamic effect of slab discontinuity on underground moving trains. In *11th International Congress on Sound and Vibration*, (2004), pp. 3045–3054.

[6] C.-X. Shi, Q. Yang, and Z.-Y. Guo. Mechanical analysis on cement concrete pavement in highway tunnel under moving load. *Journal of Highway and Transportation Research and Development*, **10**, (2008), pp. 22–25.

[7] Q. Yang, Z.-Y. Guo, and L.-P. Chen. Stress analysis of compound pavement in road tunnel considering level loads. *Journal of Highway and Transportation Research and Development*, **23**, (2006), pp. 16–19.
[8] D. Clouteau and G. Degrande. *Three-dimensional modelling of free field and structural vibration due to harmonic and transient loading in a tunnel*. Katholieke Universiteit Leuven Press, (2003).
[9] K. J. Bathe. *Finite element procedures*. Prentice Hall International, Inc Press, (1996).
[10] J. N. Reddy. *Mechanics of laminated composite plates and shells: theory and analysis*. CRC press, (2004).
[11] C. I. Bajer and B. Dyniewicz. *Numerical analysis of vibrations of structures under moving inertial load*. Springer-Verlag Berlin Heidelberg, (2012).
[12] J. A. Hernandes and R. T. Melim. A flat shell composite element including piezoelectric actuators. In *Proceedings of 12th, Intrenational Conference on Composite Materials*, (2000), pp. 172–181.
[13] C. Ren, C. Zhang, and L. Liu. Variable structure control on active suspension of 4 DOF vehicle model. *International Journal of Information Engineering and Electronic Business*, **2**, (2), (2010), pp. 54–64.
[14] L. Frỳba. *Vibration of solids and structures under moving loads*. Thomas Telford, (1999).